

Future pattern of Asian drought under global warming scenario

Do-Woo Kim · Hi-Ryong Byun

Received: 27 June 2008 / Accepted: 18 December 2008 / Published online: 22 January 2009
© Springer-Verlag 2009

Abstract This study investigates the effect of global warming on drought patterns over Asia at the end of the twenty-first century by a multi-model ensemble method based on daily precipitation data of 15 coupled climate models simulations under SRES A1B scenario, thereby assessing the consistency of responses among different models. The projected precipitation climatology was translated into the change in drought climatology using the effective drought index. The results of the models were consistent in that they project an increase in the mean and the standard deviation of precipitation over most of Asia, and the increase was considerably greater in higher latitude areas. Therefore, it is expected that in future, drought over most of Asia will occur less frequently with weaker intensity and shorter duration than those prevalent currently. However, two special regions were detected. One was the Asian monsoon regions (AMRs: South Asia and East Asia), which showed a greater increase in the standard deviation of precipitation than the mean precipitation, with an amplified seasonal precipitation cycle. As a result, part of the AMRs exhibited slight increases in drought properties such as frequency and intensity. The other region was West Asia. The region showed decreased mean precipitation, especially in its northern part (Syria and its vicinity), and more frequent droughts were projected for this region with enhanced drought intensity and lengthened drought duration. The worsening

trends in drought patterns over both regions were more significant in extreme drought, the likelihood of which is relatively higher in summer in West Asia and from spring to summer in the AMRs.

1 Introduction

Drought is amongst the world's costliest disasters and affects a very large number of people every year (Wilhite 2000). Hence, it is important to determine what increases in the frequency or severity of drought might be caused by climate change by increasing levels of greenhouse gases. Many scientists have performed experiments to study this subject by using general circulation models (GCMs). Their projections for the Asian region can be classified into three broad categories.

The first category deals with the global soil moisture condition (Manabe et al. 1981; Manabe and Wetherald 1987; Wetherald and Manabe 1999, 2002; Manabe et al. 2004). The popular projection is that soil moisture will decrease in summer while it will increase in winter over extensive regions of both the Eurasian and North American continents in high and middle latitudes. The mechanisms of these changes are based on the Clausius-Clapeyron relationship (Wetherald and Manabe 2002). As the air temperature rises, the increase in the saturation vapor pressure is much larger in the warm state than in the cool one. As a result, an increase in evaporation in summer (winter) across the middle and high latitudes is greater (smaller) than the general increase in precipitation, thereby causing drying (wetting). In the Asian area, these responses are relatively clear in central to western North Asia. Because the winter wetness is more dominant than the summer dryness, there is an overall wetting trend if the

D.-W. Kim · H.-R. Byun (✉)
Department of Environmental Atmospheric Sciences,
Pukyong National University,
599-1 Daeyeon 3-dong, Nam-gu,
Busan 608-737, South Korea
e-mail: hrbyun@pknu.ac.kr

D.-W. Kim
e-mail: dow1112@nate.com

annual average is considered (Manabe et al. 2004; Wetherald and Manabe 2002). There are, however, two limitations in this category of studies. The first limitation is that the mean value of soil moisture between present-day and the future were compared in these studies. Although this comparison yielded conclusions about climatological dryness and/or wetness, it was not applicable to actual drought. The second limitation is that the magnitude and extent of summer dryness in the middle to high latitudes in Asia are considerably different in each study. In addition, a representative response is not found in the rest of Asia.

The second category focuses on the variability of precipitation. Projections showed that over Asian monsoon regions, increases in greenhouse gas concentrations lead not only to increase in mean precipitation but also to significant enhancement in precipitation variability from sub-seasonal to inter-annual timescales (e.g., Kitoh et al. 1997; Lal et al. 2000; Hu et al. 2000; Kimoto et al. 2005). The significance of these findings was verified by recent studies using the multi-model ensemble (MME) method (Kimoto 2005; Kripalani et al. 2007a, b). The results showed that the frequency of non-precipitation increases similar to the frequency of heavy rainfall (Kimoto et al. 2005). Excess and deficiency of monsoon are also projected to intensify (Kripalani et al. 2007a). However, it remains to be understood how drought patterns are affected by enhanced variability of precipitation. In southern Europe and central North America, it has been reported that the frequency of drought will be greater by one-third and two-third, respectively, due to enhanced precipitation variability (Gregory et al. 1997).

In the third category, drought patterns obtained in GCM experiments were assessed using the palmer drought severity index (PDSI; Palmer 1965). The results suggested that the number of drought months will multiply ten times in the United States (Rind et al. 1990) and three-fold in eastern Australia (Kothavala 1999). It is reported that the dramatic worsening trend will also be observed in most of Europe (Jones et al. 1996). On a global scale, the extent, duration, and number of severe drought events are projected to increase (Burke et al. 2006). However, the projection for the Asian region (wetting trend in eastern Asia and drying trend in western Asia) in Burke et al. (2006) is contradictory to the results of previous studies on annual soil moisture (Manabe et al. 2004; Wetherald and Manabe 2002); making the validity of the previously mentioned projection debatable.

These studies have the following limitations, which must be considered for future studies on Asian drought. First, studies that investigated the average change in global soil moisture and PDSI did not consider the effect of enhanced precipitation variability. Their interest was on global-scale response; therefore, they did not consider regional features in precipitation climate change. Moreover, they used

monthly or annual data to estimate the likelihood of drought. The enhancement in precipitation variability implies that the frequency of precipitation will reduce while the intensity of precipitation will increase. Hence, the amount of precipitation tends to converge in the short term, and the number of non-precipitation or less-precipitation days might increase. In the case of droughts occurring in this situation, monthly or annual time-scale analysis is not suitable. For example, if heavy rainfall occurs on 1 July and 31 August and the interval contains non-rainfall days, the drought caused by this 60-day dry spell will not be detected by a monthly time scale analysis. Finally, most of the studies derived inferences based on a single model simulation. The levels of soil moisture or PDSI are determined by the intricate interplay between precipitation, temperature, evaporation, runoff, and soil-water holding capacity. Hence, responses to global warming obtained in these studies are more sensitive to the host model's inherent characteristics rather than precipitation or temperature response (Mitchell and Warrilow 1987; Wang 2005). The MME averaging approach can be very useful in reducing uncertainties related to model dependence. Although this method is widely used to investigate future climate patterns, it was used in a study by Wang (2005) to find the likelihood of future drought. Wang (2005) used 15 state-of-the-art GCMs. However, this study also considered soil moisture and not drought; moreover, it involved the use of monthly data.

This study examines the impact of greenhouse gas warming on Asian drought patterns by comparing the projected climate (2081~2100) in the SRES A1B experiment with the present-day control climate (1981~2000). To overcome the limitations already listed, the projected daily precipitation data are translated into drought climatology by using the effective drought index (EDI; Byun and Wilhite 1999), which quantifies the drought intensity in daily time steps. Like Wang (2005), we used the MME average from 15 GCMs and assessed its roughness. The primary focus of this study is on drought climatology (frequency, intensity, duration, and seasonality), but changes in precipitation climatology (mean, variability, and seasonal cycle) are also analyzed as important forcings for drought changes.

2 Models and methodology

2.1 Models

The GCMs used in this analysis are part of the IPCC data archive at the Lawrence Livermore National Laboratory. This collection of state-of-the-art models from international centers is being used for the IPCC's 4th Assessment Report (AR4) and consists of GCMs from more than a dozen institutes. For our study, we used 15 models for which daily

precipitation data are available (Table 1). Model characteristics for all components and other details are available at http://www-pcmdi.llnl.gov/ipcc/model_documentation/.

Two time periods of 20 years each were chosen for analysis: the late twentieth century (1981–2000; referred to as “20C3M” hereafter) and the late twenty-first century (2081–2100; referred to as “A1B” hereafter). The late twentieth century interval is considered to have modern or current climate and represents radiative forcing, consistent with observed greenhouse gas concentrations, solar variability, and volcanic forcing. The climate in the twenty-first century interval represents the simulated climate since the system was forced with rising levels of greenhouse gases, according to the SRES A1B scenario (Nakićenović et al. 2000). This emission scenario assumed a nearly linear increase in atmospheric CO₂ concentration to 720 ppm by year 2100, along with a near-linear rise in N₂O concentration and an increase in CH₄ that peaks in year 2050.

In addition to the differences in parameterization of physical and dynamical processes, the models also differ one from another in spatial resolution. The resolutions of the 15 modes range from coarse (e.g., 4°×5° for the GISS-AOM) to fine (e.g., 1.4°×1.4° in CCSM3 and finer in MIROC3.2 (hires)). To obtain the MME (average of 15 models) pattern, the original model outputs were converted to the same resolution (2.5° longitude/latitude) by employing the bi-linear interpolation technique.

Several studies have demonstrated that these models are capable of reproducing the temporal and spatial features of the precipitation climate over the Asian monsoon regions (Min et al. 2004; Kitoh and Uchiyama 2006; Kripalani et al. 2007a, b). Figure 1 shows spatial patterns of mean precipitation derived from Climate Prediction Center

Merged Analysis Precipitation (CMAP 1981-2000 period; Xie and Arkin 1997) and MME of 20C3M experiments. A visual comparison reveals that the models are able to capture the major spatial features reasonably well, except the region of the Tibetan Plateau where the models overestimate precipitation. The Tibetan Plateau region was excluded from our main focus regions in Asia as shown in Fig. 4.

2.2 Drought index

In this study, drought examination was carried using daily precipitation data. The estimation of drought features is based on the method proposed by Byun and Wilhite (1999). In that method, a new concept of drought index was proposed to solve the weaknesses of other current drought indices and to improve drought monitoring. The new features in this method are the use of daily precipitation height values and the introduction of a new concept, effective precipitation (EP), which is the summed value of daily precipitation with a time-dependant reduction function. Thus, the only data required for the calculation of the drought index were daily precipitation height values. The EP, which represents the daily depletion of water resources, was calculated using the following equation:

$$EP_i = \sum_{n=1}^i \left[\left(\sum_{m=1}^n P_m \right) / n \right] \tag{1}$$

where P_m is the precipitation m days before and index i represents the duration of summation (DS) in days. Here $i = 365$ was used, that is, summation for a year, the dominant precipitation cycle worldwide. EP_{365} can then be a representative value of the total water resources available

Table 1 List of GCMs used in this study

| Model ID | Modeling group, country | Resolution |
|------------------|--|------------|
| CCSM3 | National Center for Atmospheric Research, USA | T85 |
| CGCM3.1(T47) | Canadian Centre for Climate Modelling & Analysis, Canada | T47 |
| CGCM3.1(T63) | Same as above | T63 |
| CNRM-CM3 | Meteo-France/Centre National de Recherches Meteorologiques, France | TL63 |
| CSIRO-Mk3.0 | CSIRO Atmospheric Research, Australia | T63 |
| ECHAM5/MPI-OM | Max Planck Institute for Meteorology, Germany | T63 |
| FGOALS-g1.0 | LASG/Institute of Atmospheric Physics, China | T42 |
| GFDL-CM2.0 | Geophysical Fluid Dynamics Laboratory, USA | 2×2.5 |
| GFDL-CM2.1 | Same as above | 2×2.5 |
| GISS-AOM | NASA/Goddard Institute for Space Studies, USA | 3×4 |
| GISS-ER | Same as above | 3×4 |
| INM-CM3.0 | Institute for Numerical Mathematics, Russia | 4×5 |
| MIROC3.2(hires) | Center for Climate System Research (University of Tokyo), National Institute for Environmental Studies and Frontier Research Center for Global Change (JAMSTEC), Japan | T106 |
| MIROC3.2(medres) | Same as above | T42 |
| MRI-CGCM2.3.2 | Meteorological Research Institute, Japan | T42 |

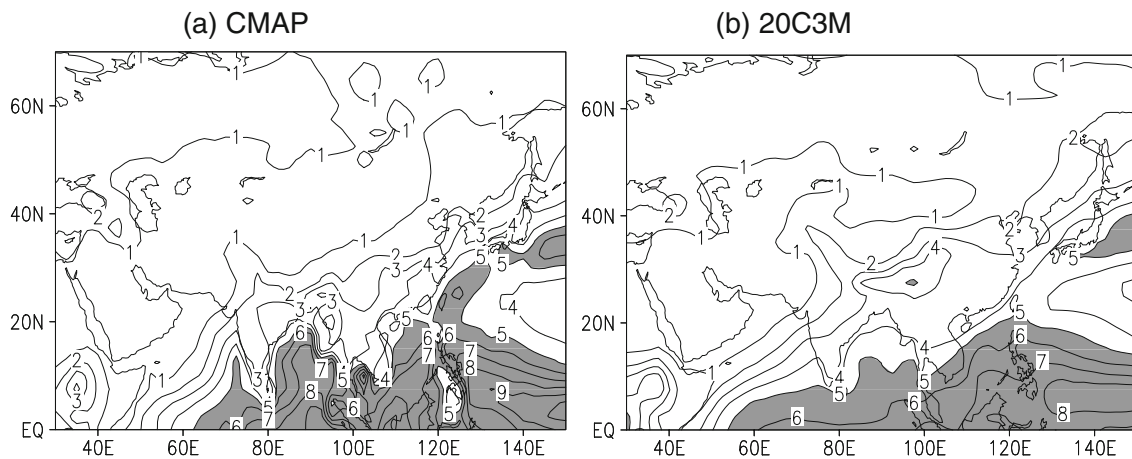


Fig. 1 Spatial pattern of mean precipitation (mm day^{-1}). **a** Observations (*CMAP*). **b** Multi-model ensemble for the present day of the *20C3M* experiments

or stored for a long time. For the calculation of EP, various equations have been proposed, but Eq. (1) is the most appropriate to represent the depletion of water resources (Lee 1998; Shim et al. 1998).

Once the daily EP is computed, a series of indices can be calculated to highlight different characteristics of a station's water resources. The first step is the calculation of mean effective precipitation (MEP), which is the climatological mean of EP for each calendar day. The MEP signifies the climatological mean of stored water quantity.

The second step is to calculate the deviation of EP (DEP) from MEP:

$$\text{DEP} = \text{EP} - \text{MEP} \quad (2)$$

DEP shows deficiency or surplus of water resources for a particular date and place.

The next step is the calculation of the standardized value of DEP (EDI):

$$\text{EDI} = \text{DEP} / \text{ST}(\text{DEP}) \quad (3)$$

where $\text{ST}(\text{DEP})$ denotes the standard deviation of each day's DEP. EDI expresses the standardized deficit or surplus of stored water quantity (Table 2). It enables one location's drought severity to be compared to that of another location, regardless of climatic differences. The

Table 2 Categorization of EDI values

| Class | EDI |
|----------------|--------------|
| Extremely wet | ≥ 2.0 |
| Very wet | 1.0 to 2.0 |
| Moderately wet | 0.5 to 1.0 |
| Normal | -0.5 to 0.5 |
| Moderately dry | -1.0 to -0.5 |
| Severely dry | -2.0 to -1.0 |
| Extreme dry | ≤ -2.0 |

use of EDI has been tested in several drought studies (Byun and Lee 2002; Yamaguchi and Shinoda 2002; Kang and Byun 2004; Kim and Byun 2006; Morid et al. 2006; Smakhtin and Hughes 2007; Akhtari et al. 2008).

When using EDI to explore the changes in drought as a result of future climate scenarios, the calibration factors were set at present-day values (Eqs. 4 and 5):

$$\text{EDI}_{20C3M} = (\text{EP}_{20C3M} - \text{MEP}_{20C3M}) / \text{ST}(\text{DEP}_{20C3M}) \quad (4)$$

$$\text{EDI}_{A1B} = (\text{EP}_{A1B} - \text{MEP}_{20C3M}) / \text{ST}(\text{DEP}_{20C3M}) \quad (5)$$

2.3 Consistency index

When the direction of hydrological changes is determined with the base of all-model averages, it will be unavoidably biased toward models with higher climate sensitivity. In extreme cases where an overly sensitive model projects a wetter condition while all others project a drier condition or vice versa, the multiple model average may reflect qualitatively the results from that one exception instead of those from the majority of the models. Consequently, a simple all-model average could yield misleading results. Therefore, instead of studying hydrological response based solely on all-model averages, we used the consistency index (Wang 2005) to quantify the level of consistency among different models in predicting the direction of responses. The consistency index is calculated as follows.

$$\text{Consistency index} = \begin{cases} \frac{N_p}{N_p + N_n} (N_p > N_n) \\ -\frac{N_n}{N_p + N_n} (N_p < N_n) \end{cases} \quad (6)$$

N_p is the number of models that project an increase in the quantity of interest and N_n is the number of models that

project a decrease. Therefore, the sign of the consistency index indicates the direction of changes projected by the majority of the models, and the magnitude of the consistency index reflects the level of majority, which is always larger than 50%.

3 Future precipitation climatology

3.1 Change in mean precipitation

Figure 2a shows the MME difference in mean annual precipitation between the A1B and the 20C3M. The annual precipitation is projected to increase over major parts of Asia. Significant increase of more than 100 mm is observed over parts of Russia, eastern China, Korea, Japan, southern India, and the Indochina peninsula. On the other hand, the annual precipitation decrease is the dominant response over middle to northern portion of West Asia. To quantify the increase in precipitation, the percentage difference is illustrated in Fig. 2b. This figure reveals that the rates of increase are larger over North (15~25%), East (5~15%), and South (5~10%) Asia, in that order. Over West Asia, the decrease rates range from 0 to 25%.

Figure 2c presents the consistency index (in percentage) for projecting precipitation changes. The sign of the index reflects the direction of change projected by the majority models. The magnitude of the index indicates the percentage of the majority models. Although any percentage greater than 50% makes a majority, only areas with a majority level higher than 60% (i.e., 9 or more out of 15 GCMs) are shaded. The distribution pattern of the consistency index is characterized by high absolute values exceeding 60%, except the narrow boundary areas between the positive and negative values. This indicates that the precipitation changes shown in Fig. 2a and b do not reflect the extreme biases in the minority models but the projection of the majority of models. The model consistency level is especially high in projecting the increase over much of North and East Asia and the decrease in the northern part (Syria and its vicinity) of West Asia.

3.2 Change in precipitation variability

The MME percentage difference in total variability (standard deviation) of precipitation data between the A1B and the 20C3M is illustrated in Fig. 3a, and the corresponding consistency index is shown in Fig. 3b. In accordance with the responses in mean precipitation (Fig. 2b), the variability in precipitation is projected to increase over much of Asia and decrease over parts of West Asia. At this time, however, the magnitude of increase over South and East Asia is comparable to that over North Asia, and the area of

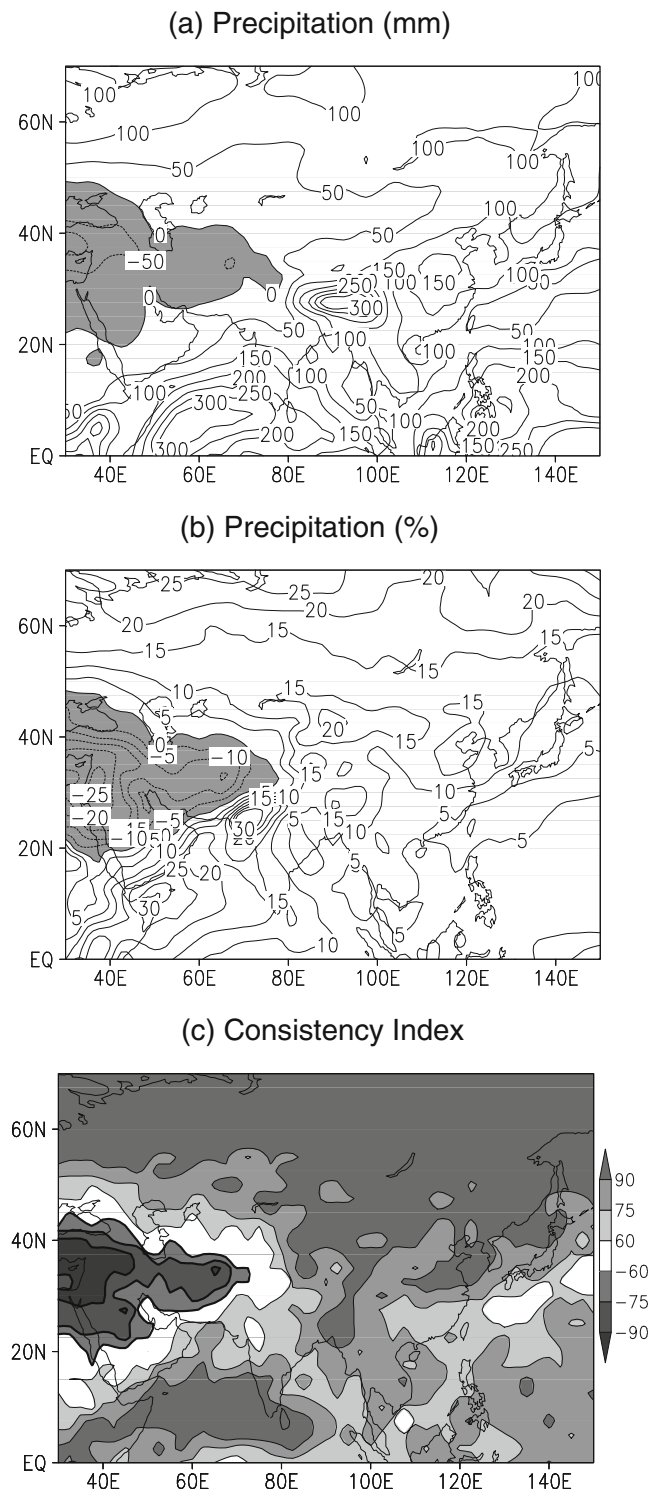


Fig. 2 Multi-model ensemble **a** difference and **b** percentage difference in mean annual precipitation between the SRES A1B experiments and the 20C3M experiments. The percentage difference is defined as $100 \times (A1B - 20C3M) / 20C3M$. **c** Consistency index (in %) of the 15 models in predicting the direction of change in mean annual precipitation

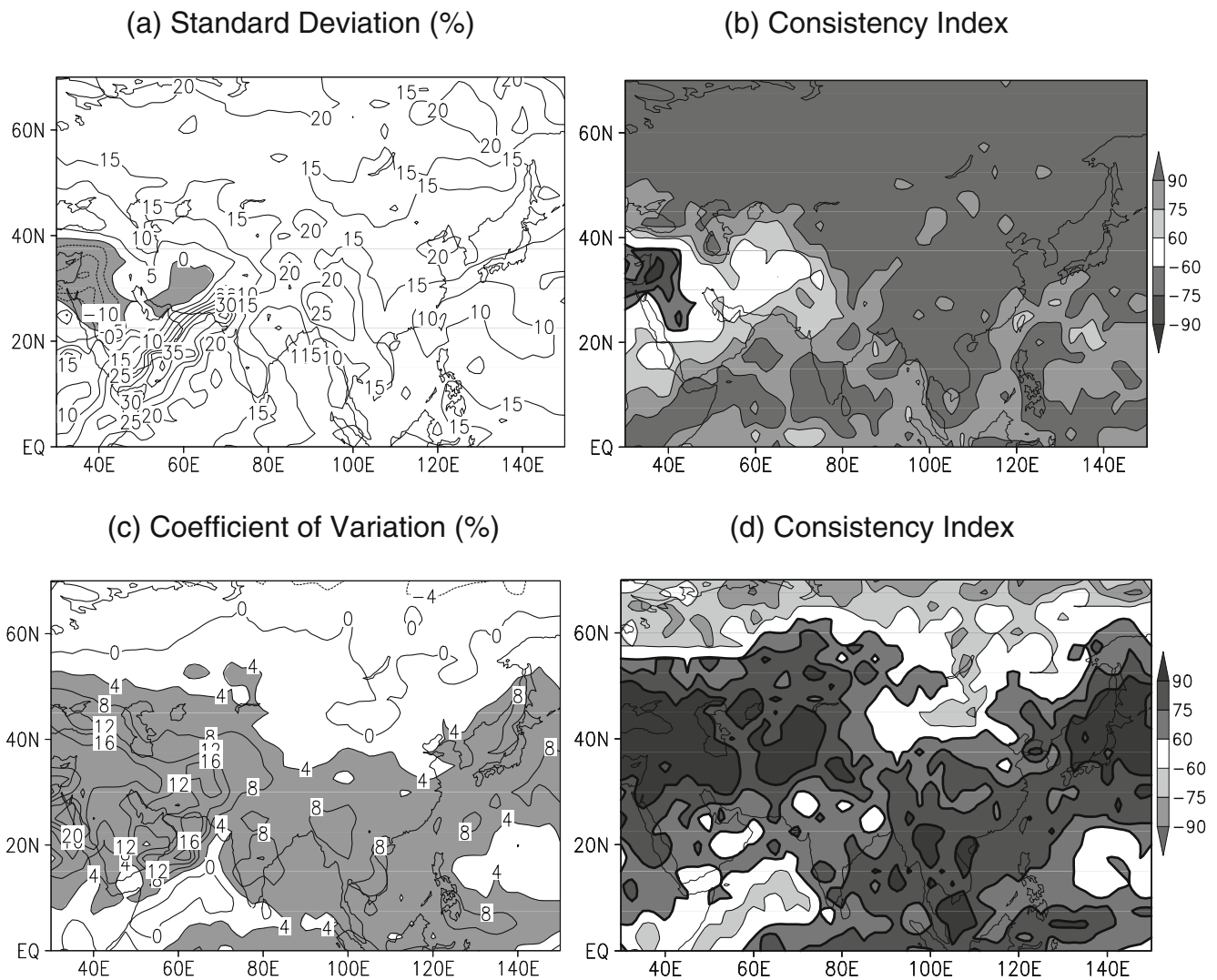


Fig. 3 Same as Fig. 2, but for percentage difference in **a–b** standard deviation and **c–d** coefficient of variation of precipitation data between the SRES A1B experiments and the 20C3M experiments

decrease in West Asia is much smaller. On comparing Fig. 3b with Fig. 2b, it is notable that over South Asia and East Asia (Asian monsoon regions; AMRs) the increase in the variability is a more consistent response among the 15 GCMs than that in the mean. Over West Asia, on the other hand, the decrease in the variability is a less congruous response than that in the mean.

Figure 3c shows the MME percentage difference of the coefficient of variation (CV; the ratio of the standard deviation to the mean) of precipitation data between the A1B and the 20C3M. Areas with an increase greater than 4% are shaded. The CV is projected to increase over the extensive area except North Asia. A relatively large increase in the CV is observed across West, South, and East Asia. The consistency level is especially high in northern West Asia and along the coastal regions in the AMRs (Fig. 3d). Through those four figures, we can find

that among regions where the mean precipitation increases, the enhancement of the precipitation variability is more significant over the AMRs. The decrease in mean precipitation accompanied by the weakening of variability (decreased standard deviation) is shown only in the small northern portion (Syria and its vicinity) of West Asia.

3.3 Change in seasonal precipitation cycle

To analyze changes in seasonal precipitation cycle over the Asian sub-regions, we divided the Asian area into North, South, West, and East Asia (Fig. 4) according to climatology as reported in the IPCC report (McCarthy et al. 2001): North Asia (boreal climate: 50–70°N, 40–130°E), South Asia (tropical climate: 10–25°N, 70–120°E), West Asia (arid and semi-arid climate: 15–45°N, 30–70°E), and East Asia (temperate climate: 25–45°N, 110–145°E).

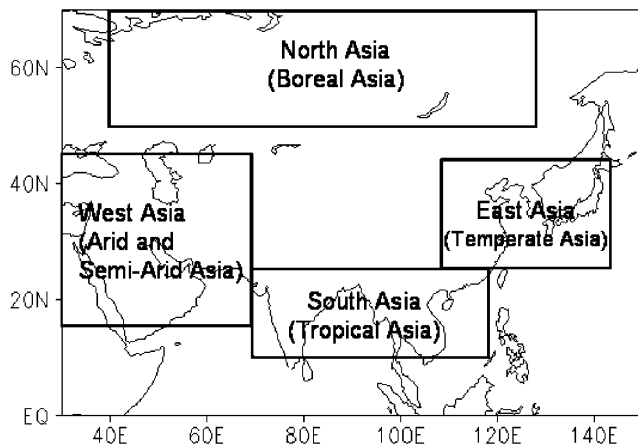


Fig. 4 Asian sub-regions: North Asia (50–70°N, 40–130°E), South Asia (10–25°N, 70–120°E), West Asia (15–45°N, 30–70°E), and East Asia (25–45°N, 110–145°E)

The MME pattern of the projected (A1B) and simulated (20C3M) seasonal cycles for the area-averaged precipitation are shown in Fig. 5. The difference in percentage between the two experiments is presented in a bar graph.

The corresponding consistency index is denoted by a cross. The error bar depicts the range of uncertainty from model differences (\pm SD of 15 GCM results). In North Asia (Fig. 5a), the models are highly consistent in projecting an increase throughout the year, reaching a consistency level to 100% for 9 out of 12 months. The magnitude of increase is especially large during the colder months. There is no month in which the response shows a decrease, even if negative ranges of model uncertainty are applied. It is therefore unlikely that the North Asian drought will intensify, at least by changes in the seasonal precipitation cycle.

West Asia, the arid and semi-arid region of Asia, has no clear seasonal cycle with very little precipitation throughout the year. Figure 5b reveals that the unreliability of the MME seasonal projection in West Asia is greater than that in the other regions. This is because the model constancy level is less than 80% for 6 months and the ranges of model uncertainty are much larger than the magnitude of the MME differences. Overall, nevertheless, a decrease is a more dominant and reliable response, and it appears from January to July. We can infer that over West Asia, which is

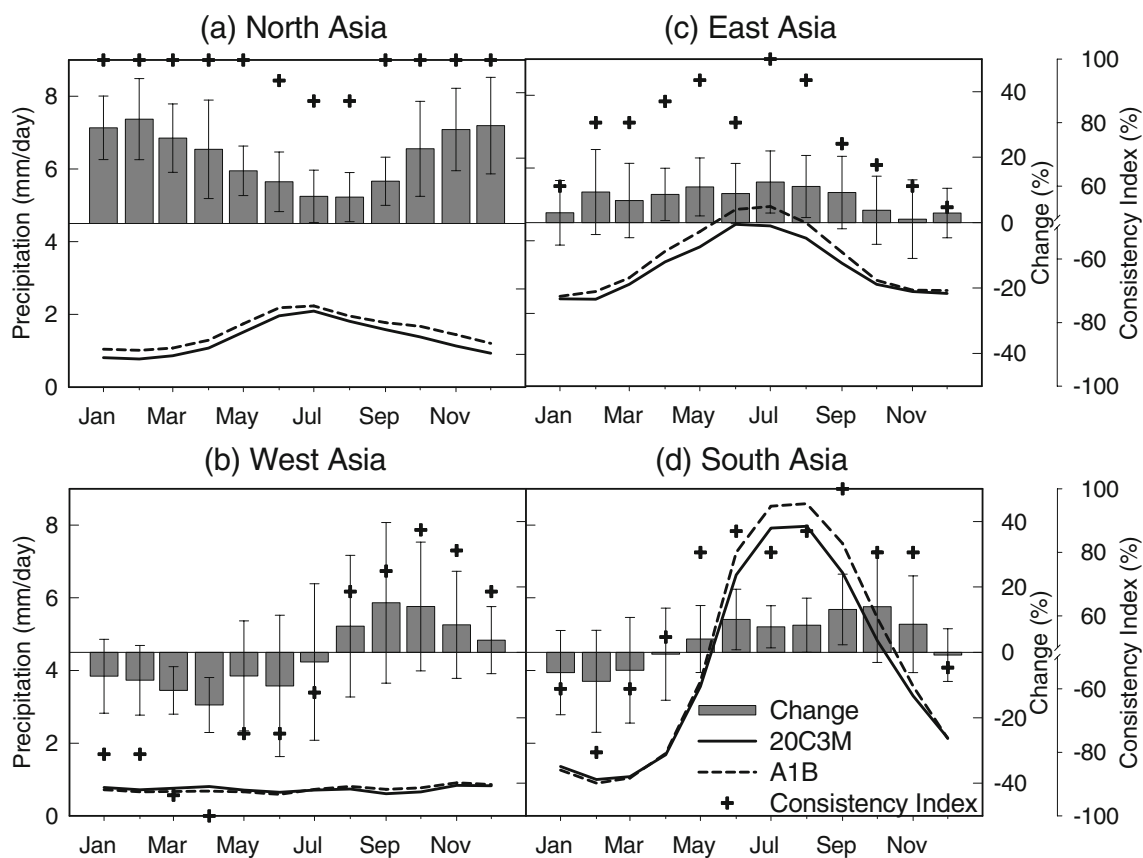


Fig. 5 Multi-model ensemble monthly mean precipitation (mm/day) for the 20C3M experiments (solid line) and the A1B experiments (dash line) depicting the annual precipitation cycle, and the percentage differences (bars) between the two experiments for each month. Inter-

model variability (standard deviation of 15 GCMs' results) and consistency index for each monthly change is depicted by an error bar and a cross mark, respectively

already dry, water stresses are likely to increase, especially during the summer season, due to the insufficient accumulated rainfall from the preceding months.

In the AMRs (East Asia and South Asia, Fig. 5c and d), a substantial increase of more than 10% is projected during the summer months with a high level of model consistency, possibly implying the strengthening of the summer monsoon. This considerable increase is not simply a summer feature but extends into the preceding spring in East Asia and into the following autumn in South Asia. The consistency level is relatively low during the colder months in both regions. Although there is an increase and a decrease in the respective winter responses in East and South Asia, the changes are not clear as compared to the corresponding ranges of model uncertainty. Because of this, the likelihood of drought cannot be excluded despite the increased mean annual precipitation in these regions. Analyses of precipitation climatology reveal nothing more than the possible changes in drought conditions. The actual changes in frequency, intensity, duration, and seasonality of drought are discussed further in section [Future drought climatology](#).

4 Present-day drought climatology

Before drought climatology in the future is analyzed, we first examined the present-day climatology of drought simulated by the 15 models. Drought was described in terms of frequency, intensity, and duration, based on the MME method. A drought event was defined as the value of the minimum EDI smaller than -1.0 . Onset was defined as the date when the EDI drops below -0.5 , and secession, as the date when EDI exceeds this value last, maintaining a negative value after onset. Duration was defined as a period between onset and secession dates and intensity as the minimum EDI during the duration.

An example of defining the three drought variables using the EDI time series is shown in Fig. 6. Precipitation and

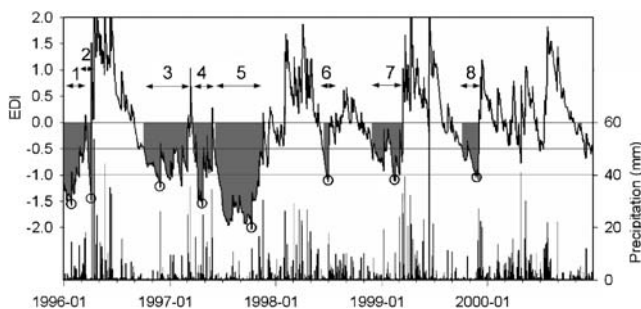


Fig. 6 Example of defining the frequency, intensity, and duration of drought using CCSM3 data at 35°N , 125°E from 1996 to 2000. *Upper time-series* is the EDI and *bottom bar* is precipitation. *Double arrow* and *open circle* indicate respectively the duration and the intensity of drought event

calculated EDI data at 35°N and 125°E for last 5 years in CCSM3 20C3M were randomly selected. At this grid point for 20 years, there were a total 23 drought events (not shown), and this figure shows that 8 out of these 23 events occurred in the last 5 years. Double arrows and open circles denote the durations and the intensities of each drought event. In Fig. 6, the mean frequency is 1.6/year, the mean intensity is the mean of 8 EDI values represented by open circles, and the mean duration is the mean of the 8 durations represented by numbered double arrows.

Figure 7 shows the MME horizontal patterns of the mean frequency, mean intensity, and mean duration of drought events in the 20C3M. In the present-day climate, the GCMs simulated that drought occurs at an average rate of $0.8\sim 1.2$ /year over a major part of Asia, with a notable exception being the Arabian Peninsula, which showed relatively low frequencies of 0.4 /year. Mean intensities were about -1.5 of EDI in most areas, but were also weak in the Arabian Peninsula. The mean durations were about 120 days but longer, up to 280 days, in the Arabian Peninsula. These results reveal that over the southern West Asia, an arid region, intensive drought occurs less frequently than in other regions but tends to last longer.

5 Future drought climatology

5.1 Change in general drought

Figure 8 shows the plot of MME differences between the three drought variables in the A1B and the 20C3M. The left panels show changes in the mean frequency, mean intensity, and mean duration, while the right panels show the corresponding consistency index. By comparing Fig. 8a and d with Fig. 2b and c, respectively, it is clear that the drought frequency tends to respond to the mean precipitation. It is projected that drought recurs with greater frequency over West Asia by $0\sim 0.2$ /year than in the present-day climate. This corresponds to an increase of $0\sim 50\%$ and is supported by a high degree of model consistency. On the other hand, drought is expected to occur less frequently over the rest of the Asian land mass. The decrease is comparatively large over North ($-0.6\sim -0.4$ /year) and East Asia ($-0.4\sim -0.2$ /year) where the model consistency is high. In percentage terms, these decreases are equivalent to about from 30 to 60%. A weak decrease of $-0.2\sim 0$ /year is dominant in South Asia, corresponding to a reduction of $0\sim 20\%$; the corresponding consistency level is also relatively low.

The difference pattern of the intensity (Fig. 8b) reveals that the West Asian drought, which was anticipated to be more frequent, will be more intensive. This is more apparent over the northern part of West Asia where

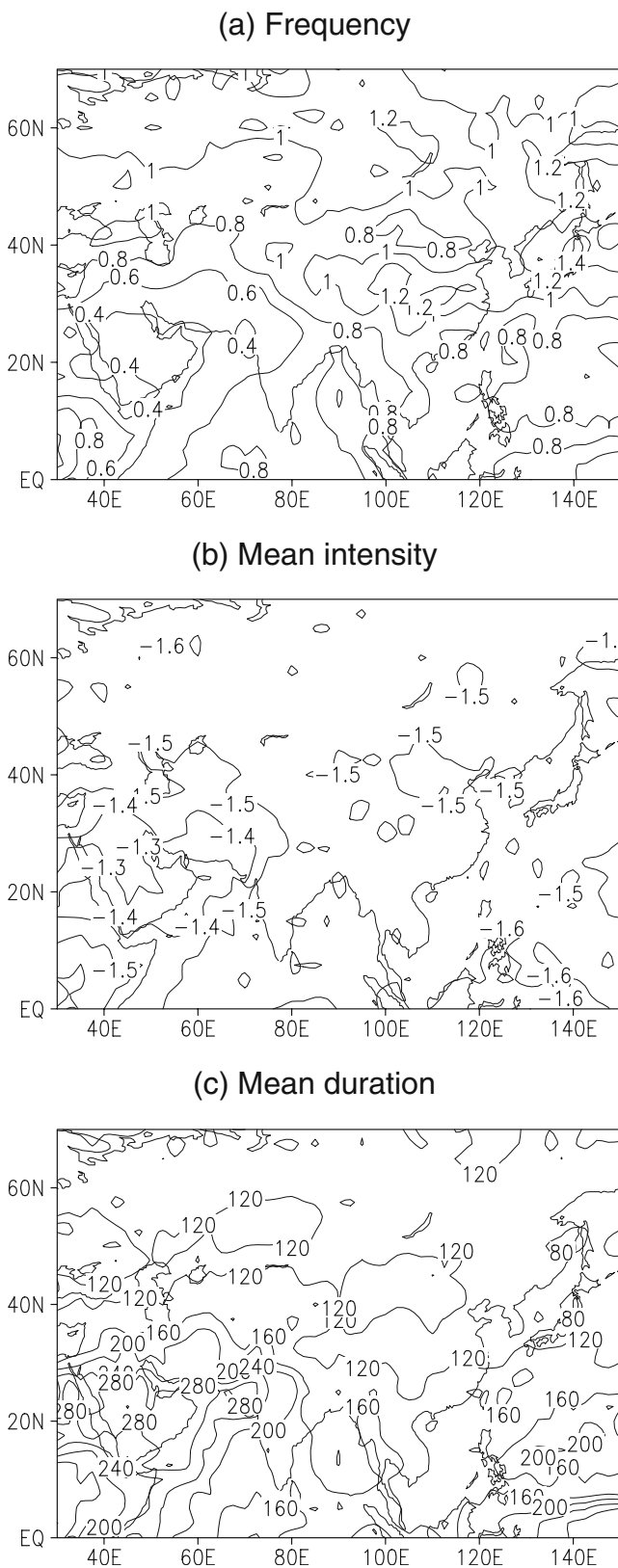


Fig. 7 Present-day drought climatology based on the multi-model ensemble average; **a** mean frequency (per a year), **b** mean intensity (minimum EDI), and **c** mean duration (days) of the drought events

precipitation largely decreases. The degree of model consistency is also high over West Asia (Fig. 8e), as good as that for the frequency. Furthermore, it is interesting to note that the intensity is projected to strengthen over the AMRs as well, in a region that showed negative frequency change, even though areas showing high consistency were confined to only some parts. The negative areas in Fig. 8b are somewhat similar to areas where the increase in the CV was beyond 4% in Fig. 3c. It is probable that significant enhancement in precipitation variability leads to intensification of drought conditions despite increased mean precipitation. On the other hand, the slight weakening trend projected with a low level of model consistency is dominant over North Asia, unlike the response of the frequency, which decreases considerably with a high consistency level.

Similarly in the case of the frequency responses, drought is projected to last for shorter durations (30~60 days) in most of Asia and longer (~120 days) in West Asia (Fig. 8c) than in the present-day climate, corresponding to 20~40% shortening and up to 60% lengthening, respectively. The degree of model consistency projecting the shortening of drought duration is especially high over the AMRs, as compared with that projecting the decrease in drought frequency. This reveals that the significant enhancement in precipitation variability over the AMRs brings about not only an increase in drought intensity but also the shortening of drought duration. On the other hand, the lengthening of drought duration, projected with a high consistency level, is only observed in the small northern part of West Asia (Fig. 8f), where both the mean and the standard deviation of precipitation decrease. The remarkable worsening trends in all of the drought variables over the northern part of West Asia imply that the Arabian Desert will expand northward.

5.2 Change in extreme drought

Because extreme drought is more dangerous, a similar diagnosis with Fig. 8 was carried out for extreme drought cases (Fig. 9). Extreme drought is defined as an event with a minimum EDI less than -2.0. Unlike the frequency response of general drought, showing an increase only over West Asia, the extreme drought frequency shows extensive increase not only over West Asia, but also over much of the AMRs (South Asia and southern part of East Asia; Fig. 9a). It is especially apparent over the northern part of West Asia, where the model consistency reaches 100% (Fig. 9d). However, that in the AMRs is less consistent results among different models. On the other hand, decreases in the frequency are still dominant over North Asia, although areas with a high consistency level are somewhat fewer.

The mean intensity exhibits a strengthening almost everywhere of Asia (Fig. 9b and e). It also shows the

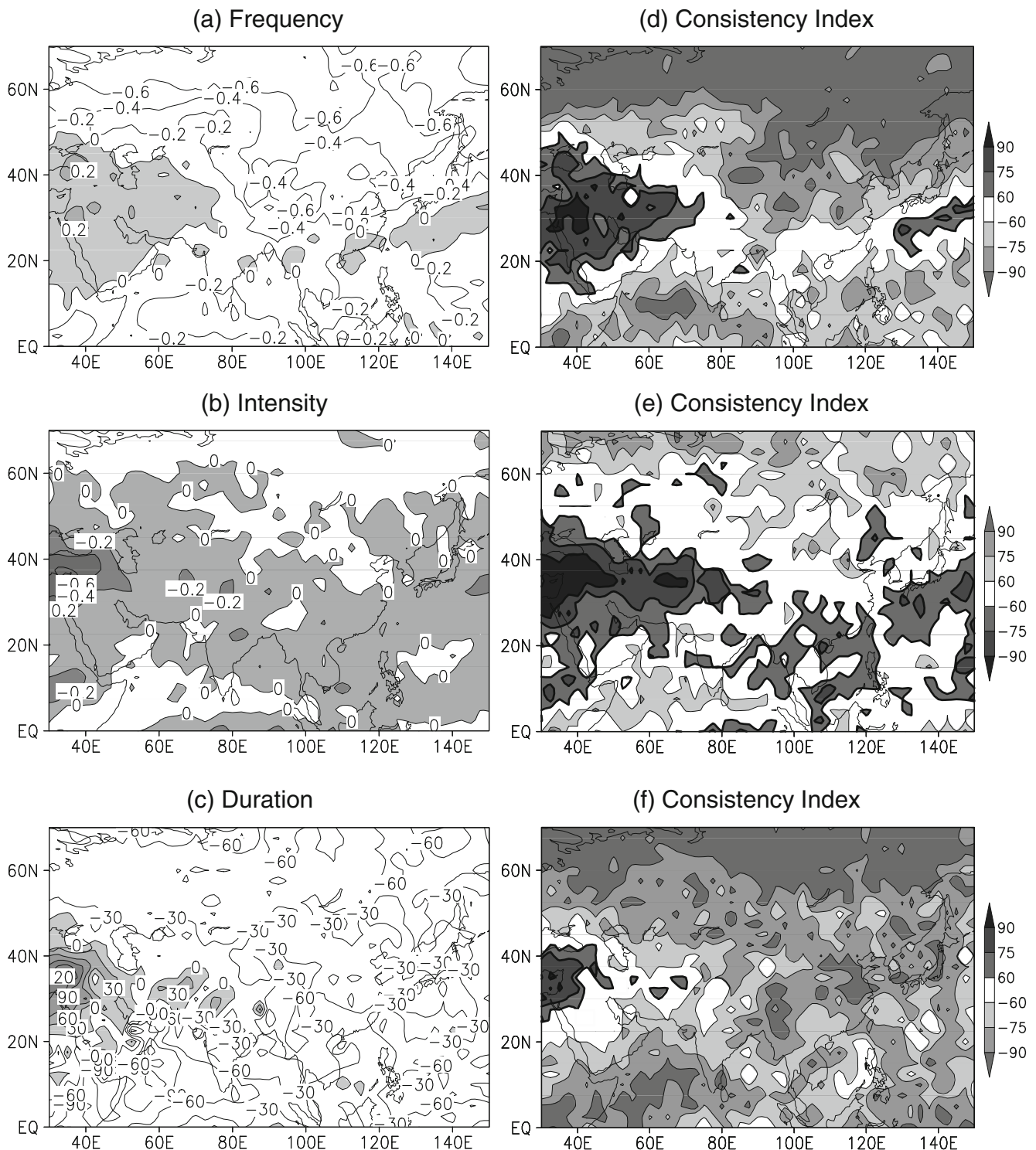


Fig. 8 Multi-model ensemble difference of **a** mean frequency (per a year), **b** mean intensity (minimum EDI), and **c** mean duration (days) of drought events between the SRES A1B experiments and the

20C3M experiments. *Right panels* represent the corresponding consistency index (%)

largest increase over northern West Asia with a high model consistency. At this time, furthermore, the increases over the AMRs are also considerable, and are accompanied by a high consistency level. It is notable that the models are

more consistent in projecting the intensification of drought over the AMRs in extreme cases than in general cases. On the other hand, the lack of model consistency is observed over most parts of North Asia.

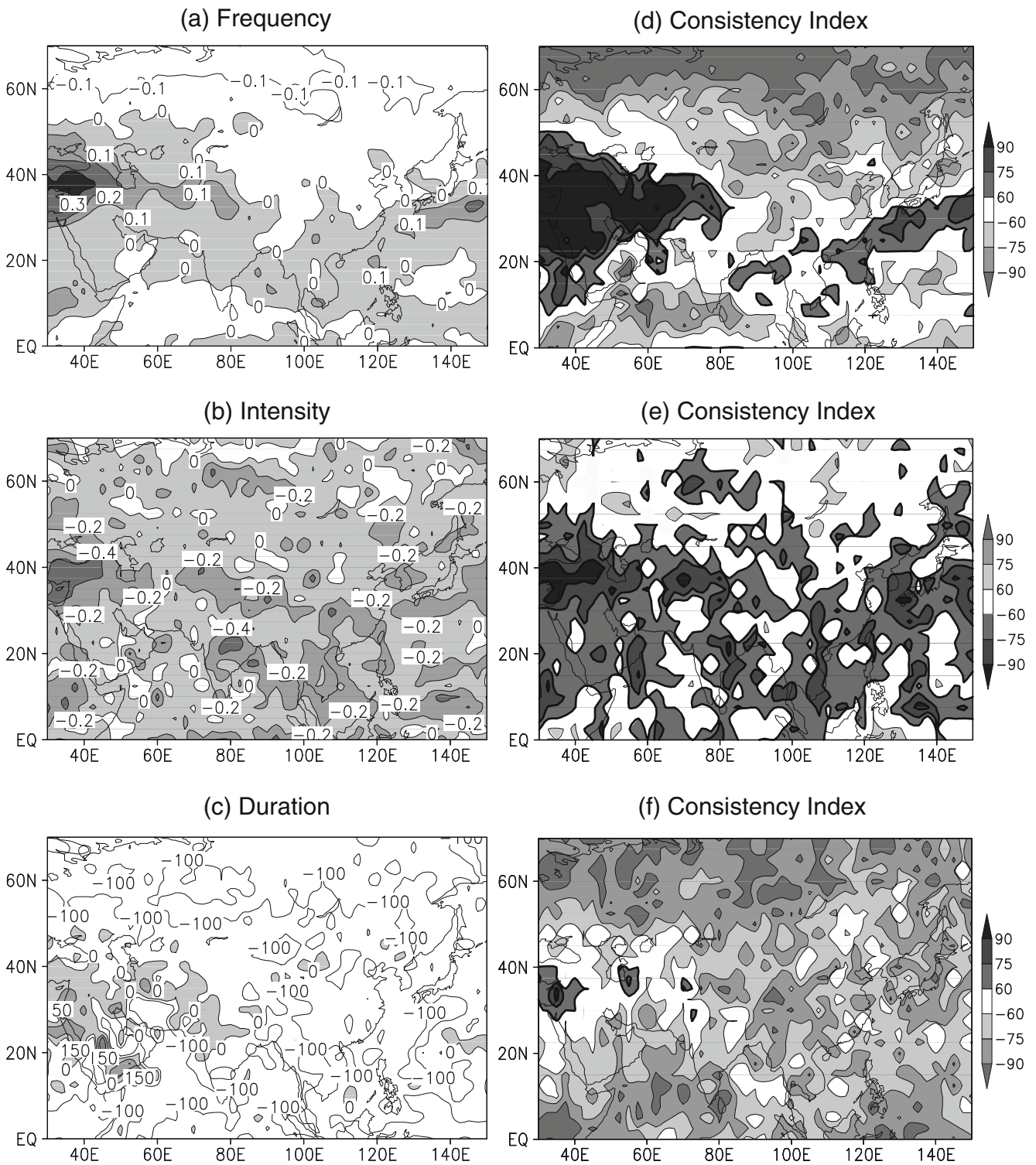


Fig. 9 Same as Fig. 8, but for extreme drought

The change in the mean duration (Fig. 9c and f) is very similar to that in general case shown in Fig. 8 c, except that the magnitude is greater. Overall, areas with a high consistency level are more widespread than those in the case of the previous two extreme drought variables.

For easier understanding, the regional changes in drought climatology shown in Figs. 8 and 9 are summarized in Table 3. Area-averaged changes in drought variables are denoted by numerals. Absolute values of greater than 60% regional averaged consistency index are

Table 3 Regional changes on drought climatology (summary of Figs. 8 and 9)

| Region | Drought | Frequency (per a year) | Intensity (EDI) | Duration (days) |
|------------|---------|------------------------|--------------------|-------------------|
| North Asia | General | -0.52 ^a | +0.03 | -46 ^a |
| | Extreme | -0.08 ^a | -0.07 | -144 ^a |
| West Asia | General | +0.08 | -0.15 ^a | 0 |
| | Extreme | +0.09 ^a | -0.16 ^a | -19 |
| South Asia | General | -0.08 | -0.09 | -33 ^a |
| | Extreme | +0.04 | -0.19 ^a | -64 ^a |
| East Asia | General | -0.15 | -0.05 | -30 ^a |
| | Extreme | +0.02 | -0.16 ^a | -74 ^a |

^a Absolute values of greater than 60% regional averaged consistency index

emphasized in bold font. The North Asian drought is expected to be less frequent and shorter, while the West Asian one is expected to be more frequent and intense. Although mitigation in drought conditions is also found in South and East Asia as well as in North Asia, it is interesting to note the intensification of extreme drought. In other words, South and East Asia could be expected to experience extreme drought with larger shortage of water resources during periods shorter than those in present-day climate conditions, in spite of the increased mean precipitation.

5.3 Change in seasonal drought

Figure 10 shows the MME difference in the total number of monthly general drought days ($-2 < EDI < -1$; upper

panels) and extreme drought days ($EDI < -2$; bottom panels) for 20 years between the A1B and the 20C3M in the Asian sub-regions. Each bar represents the area-averaged monthly difference. At the end of the bars, there are error bars that show the range of uncertainty owing to model differences and the crosses denote the consistency index. Apart from using the monthly mean drought index, which represents the monthly dryness and/or wetness, counting the number of drought days is another method to detect drought.

Overall, all regions exhibit year-round responses, but show seasonally different magnitudes in both general and extreme drought. Year-round decreases in both kinds of drought days are projected in North Asia, and this feature is more evident in the general drought case, which shows not only magnitudes of decrease greater than the ranges of uncertainty but also high consistency levels of up to -100% for 11 out of 12 months. These decreases are relatively small around September, corresponding to the low precipitation increase rate in the preceding summer, as shown in Fig. 5a.

Year-round increases in both kinds of drought days are projected in West Asia. This is more noticeable in the extreme case for which the consistency level reaches up to $+100\%$ for 8 out of 12 months, especially in summer. It can be noted that the successive precipitation decrease from January to July shown in Fig. 5b can lead to aggravated drought conditions throughout the year.

In the AMRs (South Asia and East Asia), for all seasons, the number of general drought days is projected to decrease, while the number for the extreme drought days

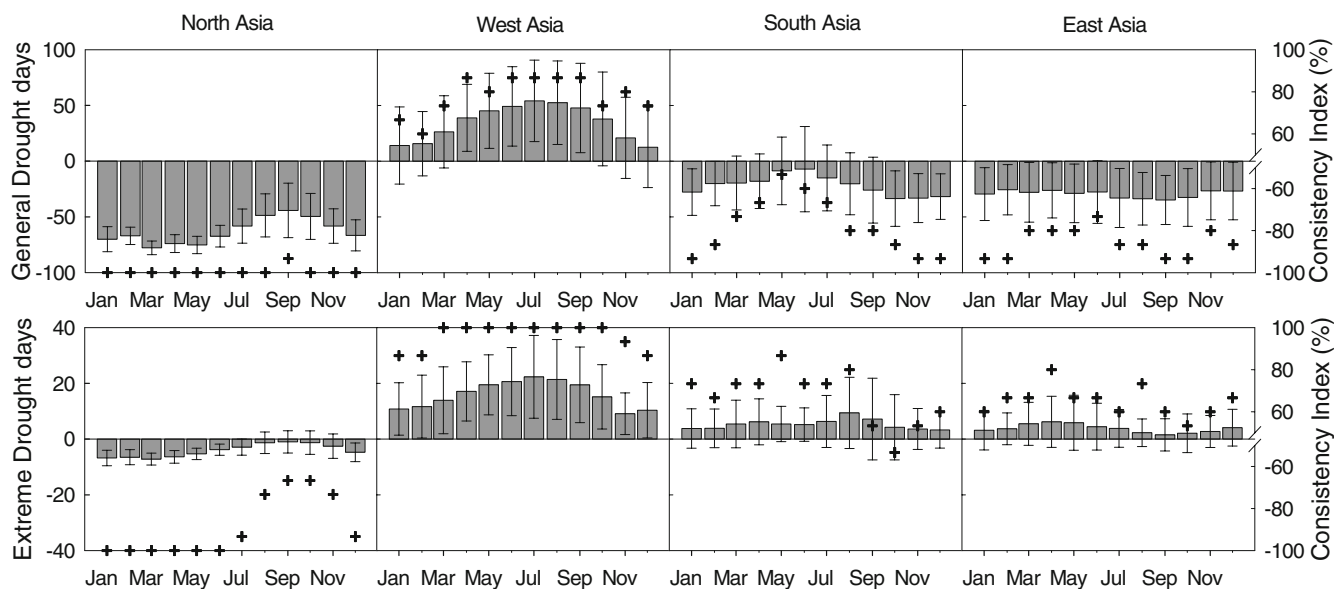


Fig. 10 Multi-model ensemble difference of area-averaged total number of monthly general ($-2 < EDI < -1$; upper panels) and extreme ($EDI < -2$; bottom panels) drought days between the SRES A1B experiments and the 20C3M experiments. Inter-model variability

(standard deviation of 15 GCMs' results) and consistency index for each monthly change is depicted by an error bar and a cross mark, respectively

is expected to increase. The year-round decrease in the general drought case in South Asia, despite the reduction in winter precipitation (Fig. 5d), could be due to the increase in summer monsoon precipitation that accounts for a considerable quantity of annual precipitation. Decreases are smaller in magnitude around May, in relation to the reduced precipitation in the preceding colder months (December–April). In East Asia, decreases in the general drought case are uniformly observed throughout the year, corresponding to the increased precipitation almost all year round, as shown in Fig. 5c. For extreme drought cases in both regions, the increase projected with the highest level of model consistency occurs in spring (May in South Asia and April in East Asia). This phenomenon seems to be affected by insufficient precipitation during the preceding colder months. The second highest consistency level is observed in August in both regions, despite the significantly greater monsoon precipitation in this month. This indicates that the enhanced variability of precipitation is also an important factor for intensifying extreme drought over the AMRs.

6 Summary and discussion

This study was the first attempt at assessing future drought patterns by focusing on the Asian region. The analysis was based on 15 GCM multiple-model ensemble averages of climate differences between present-day control simulation (1981–2000) and the SRES A1B experiment (2081–2100). To assess the robustness of the results, the consistency ratio among models was calculated. The projected precipitation climatology was translated into the change in drought climatology using the effective drought index (EDI) which quantifies the drought intensity in daily time steps.

Projections of the mean precipitation in the SRES A1B scenario revealed wetness over a large portion of Asia and dryness over West Asia. Particularly in North Asia, we found no possibility of aggravation in drought conditions. This is because the models consistently projected not only a large increase in mean precipitation for all seasons, especially in the cold months, but also insignificant changes in precipitation variability. In East and South Asia (Asian monsoon regions), however, the increase in mean precipitation was projected to be accompanied by even larger magnitudes of increase in variability, amplifying the seasonal precipitation cycle (increase in summer and decrease or insignificant change in winter). Thus, an increase in the likelihood of drought cannot be ruled out. Drought is most likely to aggravate over West Asia, due to the decrease in mean precipitation that mainly occurs from winter to summer seasons. Particularly in the northern parts of West Asia (Syria and its vicinity), the decrease is not

only considerable but is also accompanied by reduced variability.

We estimated the actual responses in the frequency, intensity, and duration of drought to the precipitation climate changes. The models were consistent in projecting worsening drought conditions in West Asia, especially in its northern part. This result was in agreement with that obtained in recent studies on future global dryness (Manabe et al. 2004; Wang 2005; Burke et al. 2006). However, we verified that there is an actual increase in the frequency and intensity of drought, even if the effect of increased evaporation due to higher air temperature was excluded. A tendency for drought to last longer is observed only over the northern part of West Asia, where both the mean and standard deviation of precipitation decreased. These worsening tendencies were more significant in summer and in the case of extreme drought.

The mitigation of drought conditions is a major response over most of Asia. Among three drought variables, the most extensive response over Asia is the shortening of the drought duration, and the second one is the reduction in the number of drought occurrences. These responses were most significant in North Asia, with slightly weakened drought intensity. Although many previous studies on soil moisture have suggested that winter and summer in North Asia show wetness and dryness, respectively (e.g., Wetherald and Manabe 2002; Manabe et al. 2004; Wang 2005), we found that drought originating from the lack of precipitation is significantly weakened in all seasons, especially in winter to spring.

The year-round weakening of drought is also projected over Asian monsoon regions. Because of the large variability of precipitation, however, the frequency of extreme drought does not significantly decrease. Furthermore, the strengthening of extreme drought intensity is a more consistent result among the different models. These features are relatively more significant during pre-monsoon and monsoon seasons.

This study revealed that drought over West Asia will worsen, especially in the northern part of the region. This implies that the Arabian Desert will be more arid and expand northward into Syria and its vicinity. Furthermore, a tendency of drought to intensify was detected over the Asian monsoon regions, despite the increase in mean precipitation. These worsening drought trends are more apparent in the case of extreme drought. This is a rather serious projection, because if increased evaporation occurs in warmer climates, future drought patterns will be much more severe than our results.

Acknowledgements We acknowledge the modeling groups, the Program for Climate Model Diagnosis and Intercomparison (PCMDI) and the WCRP's Working Group on Coupled Modelling (WGCM) for their roles in making available the WCRP CMIP3 multi-model

dataset. Support of this dataset is provided by the Office of Science, US Department of Energy. This work was funded by the Korea Meteorological Administration Research and Development Program under Grant CATER 2006-2306.

References

- Akhtari R, Morid S, Mahdian MH, Smakhin V (2008) Assessment of areal interpolation methods for spatial analysis of SPI and EDI drought indices. *Int J Climatol* 29:135–145. doi:10.1002/joc.1691
- Burke EJ, Brown SJ, Christidis N (2006) Modeling the recent evolution of global drought and projections for the twenty-first century with the Hadley Centre climate model. *J Hydrometeorol* 7:1113–1125
- Byun HR, Lee DK (2002) Defining three rainy seasons and the hydrological summer monsoon in Korea using available water resources index. *J Meteorol Soc Japan* 80:33–44
- Byun HR, Wilhite DA (1999) Objective quantification of drought severity and duration. *J Clim* 12:2747–2756
- Gregory JM, Mitchell JFB, Brady AJ (1997) Summer drought in northern mid-latitudes in a time-dependent CO₂ climate experiment. *J Clim* 10:662–686
- Hu ZZ, Latif M, Roeckner E, Bengtsson L (2000) Intensified Asian summer monsoon and its variability in a coupled model forced by increasing greenhouse gas concentrations. *Geophys Res Lett* 27:2681–2684
- Jones PD, Hulme M, Briffa KR, Jones CG, Mitchell JFB, Murphy JM (1996) Summer moisture availability over Europe in the Hadley Centre general circulation model based on the Palmer Drought Severity Index. *Int J Climatol* 16:155–172
- Kang KA, Byun HR (2004) On the developing processes of the climatological drought over the East Asia in 1982. *J Kor Met Soc* 40:467–483
- Kim YW, Byun HR (2006) On the causes of summer droughts in Korea and their return to normal. *J Kor Met Soc* 42:237–251
- Kimoto M (2005) Simulated change of the east Asian circulation under global warming scenario. *Geophys Res Lett* 32, L16701. doi:10.1029/2005GL023383
- Kimoto M, Yasutomi N, Yokoyama C, Emori S (2005) Projected changes in precipitation characteristics around Japan under the global warming. *SOLA* 1:85–88
- Kitoh A, Uchiyama T (2006) Changes in onset and withdrawal of the East Asian summer rainy season by multi-model global warming experiments. *J Meteorol Soc Japan* 84:247–258
- Kitoh A, Yukimoto S, Noda A, Motoi T (1997) Simulated changes in the Asian summer monsoon at times of increased atmospheric CO₂. *J Meteorol Soc Japan* 75:1019–1031
- Kothavala Z (1999) The duration and severity of drought over eastern Australia simulated by a coupled ocean-atmosphere GCM with a transient increase in CO₂. *Environ Model Software* 14:243–252
- Kripalani RH, Oh JH, Chaudhari HS (2007a) Response of the East Asian summer monsoon to doubled atmospheric CO₂: coupled climate models simulations and projections under IPCC AR4. *Theor Appl Climatol* 87:1–28
- Kripalani RH, Oh JH, Kulkarni A, Sabade SS, Chaudhari HS (2007b) South Asian summer monsoon precipitation variability: coupled climate model simulations and projections under IPCC AR4. *Theor Appl Climatol* 90:133–159
- Lal M, Meehl GA, Arblaster JM (2000) Simulation of Indian summer monsoon rainfall and its intraseasonal variability in the NCAR climate system model. *Reg Environ Change* 1:163–179
- Lee SH (1998) Flood simulation with the variation of runoff coefficient in tank model. *J Kor Water Resour Assoc* 31:3–12
- Manabe S, Wetherald RT (1987) Large-scale changes of soil wetness induced by an increase in atmospheric carbon dioxide. *J Atmos Sci* 44:1211–1235
- Manabe S, Wetherald RT, Stouffer RJ (1981) Summer dryness due to an increase of atmospheric CO₂ concentration. *Clim Change* 3:347–386
- Manabe S, Wetherald RT, Milly PCD, Delworth TL, Stouffer RJ (2004) Century-scale change in water availability: CO₂-quadrupling experiment. *Clim Change* 64:59–76
- McCarthy JJ, Canziani OF, Leary NA, Dokken DJ, White KS (eds) (2001) *Climate change 2001: impacts, adaptation and vulnerability*. Cambridge University Press, Cambridge, UK
- Min SK, Park EH, Kwon WT (2004) Future projections of East Asian climate change from multi-AOGCM ensembles of IPCC SRES scenario simulations. *J Meteorol Soc Japan* 82:1187–1211
- Mitchell JFB, Warrilow DA (1987) Summer dryness in northern mid-latitudes due to increased CO₂. *Nature* 330:238–240
- Morid S, Smakhtin V, Moghaddasi M (2006) Comparison of seven meteorological indices for drought monitoring in Iran. *Int J Climatol* 26:971–985
- Nakićenović N, Alcamo J, Davis G, DeVries B, Fenhann J, Gaffin S, Gregory K, Gruebler A, Jung TY, Kram T, Lebre LaRovere E, Michaelis L, Mori S, Morita T, Pepper W, Pitcher H, Price L, Riahi K, Roehrl A, Rogner H-H, Sankovski A, Schlesinger M, Shukla P, Smith S, Swart R, VanRooijen S, Victor N, Dadi Z (2000) *Special report on emissions scenarios: a special report of Working Group III of the Intergovernmental Panel on Climate Change*. IPCC, Cambridge University Press, Cambridge, UK
- Palmer WC (1965) *Meteorological drought*. Office of Climatology research paper 45. US Weather Bureau, Washington, DC
- Rind D, Goldberg R, Hansen J, Rosenzweig C, Ruedy R (1990) Potential evapotranspiration and the likelihood of future drought. *J Geophys Res* 95:9983–10004
- Shim SB, Kim MS, Shim KC (1998) Flood inflow forecasting on multipurpose reservoir by neural network. *J Kor Water Resour Assoc* 31:45–58
- Smakhtin VU, Hughes DA (2007) Automated estimation and analyses of meteorological drought characteristics from monthly rainfall data. *Environ Model Software* 22:880–890
- Wang G (2005) Agricultural drought in a future climate: results from 15 global climate models participating in the IPCC 4th assessment. *Clim Dyn* 25:739–753
- Wetherald RT, Manabe S (1999) Detectability of summer dryness caused by greenhouse warming. *Clim Change* 43:495–511
- Wetherald RT, Manabe S (2002) Simulation of hydrologic changes associated with global warming. *J Geophys Res* 107:4379–4394
- Wilhite DA (2000) Droughts as a natural hazard: concepts and definitions. In: *Drought: a global assessment* Routledge, London, pp 3–18
- Xie P, Arkin PA (1997) Global precipitation: a 17-year monthly analysis based on gauge observations, satellite estimates and numerical model outputs. *Bull Am Meteorol Soc* 78:2539–2558
- Yamaguchi Y, Shinoda M (2002) Soil moisture modeling based on multiyear observations in the Sahel. *J Appl Meteorol* 41:1140–1146